New Journal of Physics
The open access journal at the forefront of physics
Deutsche Physikalische Gesellschaft DPG
IOP Institute of Physics

PAPER • OPEN ACCESS

Anisotropic swim stress in active matter with nematic order

To cite this article: Wen Yan and John F Brady 2018 *New J. Phys.* **20** 053056

New Journal of Physics
The open access journal at the forefront of physics

Deutsche Physikalische Gesellschaft DPG
IOP Institute of Physics
Published in partnership with: Deutsche Physikalische Gesellschaft and the Institute of Physics

CrossMark

OPEN ACCESS

RECEIVED
27 February 2018

REVISED
30 April 2018

ACCEPTED FOR PUBLICATION
10 May 2018

PUBLISHED
24 May 2018

PAPER

Anisotropic swim stress in active matter with nematic order

Wen Yan[1,3,4,5] and John F Brady[2]

[1] Department of Mechanical & Civil Engineering, Division of Engineering & Applied Science, California Institute of Technology, Pasadena, CA 91125, United States of America
[2] Division of Chemistry & Chemical Engineering and Division of Engineering & Applied Science, California Institute of Technology, Pasadena, CA 91125, United States of America
[3] Current Address: Center for Computational Biology, Flatiron Institute, Simons Foundation, New York, NY 10010, United States of America.
[4] Current Address: Courant Institute of Mathematical Sciences, New York University, New York, NY 10012, United States of America.
[5] Author to whom any correspondence should be addressed.

E-mail: wyan@flatironinstitute.org and jfbrady@caltech.edu

Keywords: active Brownian particles, swim stress, normal stress difference, nematic order

Supplementary material for this article is available online

Abstract

Active Brownian particles (ABPs) transmit a swim pressure $\Pi^{\text{swim}} = n\zeta D^{\text{swim}}$ to the container boundaries, where ζ is the drag coefficient, D^{swim} is the swim diffusivity and n is the uniform bulk number density far from the container walls. In this work we extend the notion of the isotropic swim pressure to the anisotropic tensorial swim stress $\boldsymbol{\sigma}^{\text{swim}} = -n\zeta\boldsymbol{D}^{\text{swim}}$, which is related to the anisotropic swim diffusivity $\boldsymbol{D}^{\text{swim}}$. We demonstrate this relationship with ABPs that achieve nematic orientational order via a bulk external field. The anisotropic swim stress is obtained analytically for dilute ABPs in both 2D and 3D systems. The anisotropy, defined as the ratio of the maximum to the minimum of the three principal stresses, is shown to grow exponentially with the strength of the external field. We verify that the normal component of the anisotropic swim stress applies a pressure $\Pi^{\text{swim}} = -(\boldsymbol{\sigma}^{\text{swim}} \cdot \boldsymbol{n}) \cdot \boldsymbol{n}$ on a wall with normal vector $\boldsymbol{n}$, and, through Brownian dynamics simulations, this pressure is shown to be the force per unit area transmitted by the active particles. Since ABPs have no friction with a wall, the difference between the normal and tangential stress components—the normal stress difference—generates a net flow of ABPs along the wall, which is a generic property of active matter systems.

1. Introduction

In active matter each particle propels itself with a velocity U_0 along a direction characterized by an orientation vector $\boldsymbol{q}$, and by manipulating $\boldsymbol{q}$, either as a result of some intrinsic reorientation mechanism (e.g. Brownian torques) or in response to an external field, interesting phenomena arise, such as shear trapping [1], rheotaxis [2], action-at-distance [3], etc. These phenomena can be captured via particle-level Langevin dynamic simulation of the simple Active Brownian particles (ABPs) model, or by solving the corresponding Smoluchowski equation for the probability density in position and orientation space.

As a complement to the Smoluchowski analysis, continuum mechanics may also be applicable and provide a simpler description in the large-scale to determine the deformation and flow of active matter. The detailed dynamics at the Smoluchowski level are encapsulated into the balance of forces and stresses at the continuum scale—a balance of body and surface forces. The surface force of active matter is the swim pressure [4], which is the pressure required to confine the swimmers within a volume, and, like the osmotic pressure of passive Brownian particles, the swim pressure is related to the swim diffusivity: $\boldsymbol{\sigma}^{\text{swim}} = -n\zeta D^{\text{swim}}\boldsymbol{I}$, where n is the number density in the bulk and ζ is the drag coefficient. For ABPs the orientation $\boldsymbol{q}$ is governed by unbiased rotational Brownian diffusion $D_R = 1/\tau_R$. The swim diffusivity $D^{\text{swim}} = U_0^2\tau_R/6$ is isotropic. In analogy to the osmotic pressure of passive Brownian particles $\boldsymbol{\sigma}^{\text{osmo}} = -n\zeta D_T\boldsymbol{I} = -nk_B T\boldsymbol{I}$, where D_T is the thermal translational Brownian diffusivity, we define $k_s T_s = \zeta U_0^2\tau_R/6$ in 3D and $k_s T_s' = \zeta U_0^2\tau_R/2$ in 2D [4, 5].

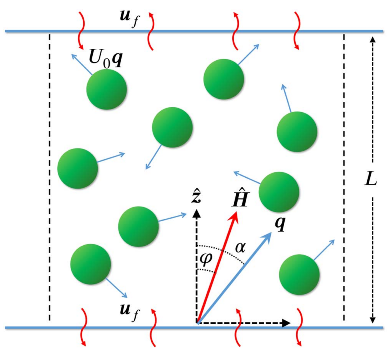

Figure 1. Sketch of the 2D geometry. The external field direction is $\hat{\boldsymbol{H}}$ and $U_0\boldsymbol{q}$ is the swim velocity of each ABP. The normal vector of the bottom wall $\boldsymbol{n} = \hat{\boldsymbol{z}}$, $\boldsymbol{q}\cdot\hat{\boldsymbol{z}} = \cos\alpha$, and $\hat{\boldsymbol{H}}\cdot\hat{\boldsymbol{z}} = \cos\varphi$.

However, if one biases the orientation with an external field along some direction $\hat{\boldsymbol{H}}$, then the swim diffusivity $\boldsymbol{D}^{\text{swim}}$ is in general anisotropic. In the case of ABPs with polar order [3, 6], the anisotropic diffusivity is superposed onto the directed net motion induced by the polar order. In the nematic case discussed in this work, the anisotropy of the diffusivity is naturally along the direction of the nematic orientation field, but directed net motion is absent. In this case, we shall demonstrate that the diffusivity increases rapidly along the nematic field direction but decreases in the perpendicular direction as the orientation field strength increases. This feature allows us to make accurate measurements and comparisons with our theory. In contrast, it is usually difficult to measure principal stresses accurately in the polar ordered case, because (i) the net motion must be canceled precisely by a body force in the opposite direction [3], and (ii) the diffusivity rapidly decreases in any direction. In the anisotropic case, it is natural to keep the definition of swim stress as a confinement stress, $\boldsymbol{\sigma}^{\text{swim}} = -n\zeta\boldsymbol{D}^{\text{swim}}$, but whether this definition is self-consistent in the mechanical sense is not known. In this work we address this question: can the swim stress be a true tensorial stress?

Without loss of generality, we consider 2D ABPs between two parallel walls separated by L as shown in figure 1 under a bistable orientational potential energy function $V(\boldsymbol{q}) = -\epsilon(\boldsymbol{q}\cdot\hat{\boldsymbol{H}})^2$, where ϵ is an energy scale. Energy is minimized for $\boldsymbol{q} = \pm\hat{\boldsymbol{H}}$; such a potential is seen for magnetic nanoparticles [7]. We define $\chi_R = \epsilon/k_B\text{T}$ as the dimensionless strength of the field. The nematic field direction is applied at an angle φ relative to the wall normal vector $\boldsymbol{n}$: $\cos\varphi = \boldsymbol{n}\cdot\hat{\boldsymbol{H}}$. Fluid is assumed to flow freely across the wall—it is an osmotic barrier—so that only the particle pressure is measured, and the wall-particle interaction is taken to be excluded volume only. The configuration is similar to the sedimentation problem [3], except that in this work we consider the dilute limit so swimmer–swimmer interactions are ignored. We also impose $L/\ell \to \infty$ to eliminate any confinement effects [5, 8], where the run-length $\ell = U_0\tau_R$.

Note that this potential creates no polar order, $\langle\boldsymbol{q}\rangle = 0$, only nematic order; $\boldsymbol{Q} = \langle\boldsymbol{qq}\rangle - 1/2\boldsymbol{I} \neq 0$. Further, since the orienting field is applied homogeneously and the wall-particle interactions are excluded volume only, issues associated with the force on a boundary differing from the bulk swim pressure [9] do not apply. Thus, for these conditions, the tensorial continuum perspective predicts a normal pressure on the wall from the anisotropic swim stress: $\Pi^{W,\text{swim}} = -(\boldsymbol{\sigma}^{\text{swim}}\cdot\boldsymbol{n})\cdot\boldsymbol{n}$.

Independent of the continuum perspective, the swim pressure on a wall has also been explained microscopically [5, 10] where ABPs accumulate in a wall boundary layer with thickness of order $\delta = \sqrt{D_T\tau_R}$. This colloidal perspective predicts $\Pi^{W,\text{swim}} = \Pi^{W,\text{tot}} - \Pi^{W,\text{osmo}} = (n^W - n)\zeta D_T$, where n^W and n are the number density of ABPs at the wall and in the bulk, respectively.

In this work we first follow the tensorial continuum perspective to calculate $\Pi^{W,\text{swim}}$ analytically. We then use the colloidal perspective to calculate $\Pi^{W,\text{swim}}$ by solving the Smoluchowski equation for the distribution $P(\boldsymbol{x}, \boldsymbol{q})$ at steady state, utilizing $n^W = \int P(\boldsymbol{x}^W, \boldsymbol{q})\mathrm{d}\boldsymbol{q}$. We show that the two perspectives agree with each other for arbitrary field direction $\hat{\boldsymbol{H}}$, and also agree with the force/area determined directly from Brownian dynamics (BD) simulations. We further show that the normal stress difference generates a net flow of ABPs along the wall.

2. The tensorial continuum (macroscopic) perspective

The swim stress $\boldsymbol{\sigma}^{\text{swim}}$ is an intrinsic property of ABPs in the bulk, regardless of the presence of a boundary. Therefore we consider only the relation between $\boldsymbol{q}$ and $\hat{\boldsymbol{H}}$ and define $\cos\theta = \boldsymbol{q}\cdot\hat{\boldsymbol{H}}$, $\theta \in [-\pi, \pi)$ for convenience. By definition $\boldsymbol{\sigma}^{\text{swim}} = -n\zeta\boldsymbol{D}^{\text{swim}}$, and $\boldsymbol{D}^{\text{swim}}$ is in general given as the time-integration of the velocity auto-correlation function (VACF). In the ABP model, since the velocity magnitude is fixed, the VACF is

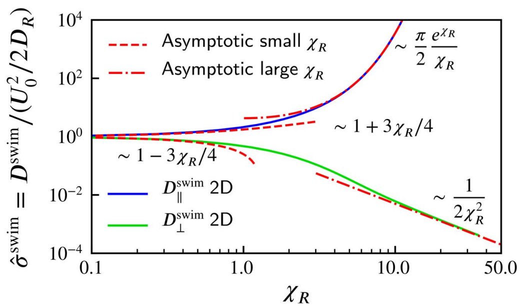

Figure 2. The swim diffusivity D^{swim} in the directions parallel and perpendicular to the external field $\hat{H}$ in 2D. The solid lines are the analytical solutions (4). Here, $\chi_R = \epsilon/k_B T$, where ϵ is the strength of the bipolar orienting potential.

simply the orientation auto-correlation function (OACF), scaled by U_0^2. The time-integration of OACF can be conveniently computed without approximation with generalized Taylor dispersion theory [11]. Quantitatively, $\boldsymbol{D}^{swim}$ can be computed with the fluctuation field $\boldsymbol{B}$ as a function of $\boldsymbol{q}$, defined as the solution to the following equation, subject to proper boundary conditions:

$$\nabla_{\boldsymbol{q}} \cdot [\boldsymbol{u}(\boldsymbol{q}) P_0^\infty(\boldsymbol{q}) \boldsymbol{B} - \boldsymbol{d}(\boldsymbol{q}) \cdot \nabla_{\boldsymbol{q}}(P_0^\infty(\boldsymbol{q})\boldsymbol{B})] = \Delta \boldsymbol{U}(\boldsymbol{q}) P_0^\infty(\boldsymbol{q}), \tag{1}$$

where $\boldsymbol{u}(\boldsymbol{q})$ is the deterministic motion of $\boldsymbol{q}$, $\boldsymbol{d}(\boldsymbol{q})$ is the diffusivity of $\boldsymbol{q}$, $P_0^\infty(\boldsymbol{q})$ denotes the equilibrium distribution, and $\Delta \boldsymbol{U}(\boldsymbol{q}) = \boldsymbol{U}(\boldsymbol{q}) - \langle \boldsymbol{U} \rangle$. Physically, $\boldsymbol{B}$ is the fluctuation field of $\boldsymbol{q}$, describing how much 'fluctuation' of $\boldsymbol{q}$ is transferred to the diffusive motion. In the 2D case discussed here, $\boldsymbol{q}$ reduces to an one-dimensional variable θ, $\boldsymbol{u}(\boldsymbol{q})$ is the angular velocity, $\boldsymbol{d}(\boldsymbol{q})$ reduces to D_R, and $\langle \boldsymbol{U} \rangle = 0$ because the nematic order does not induce net motion.

At steady state, the equilibrium distribution P_0^∞ of θ is:

$$P_0^\infty(\theta) = e^{\frac{1}{2}\chi_R \cos(2\theta)}/[2\pi I_0(\chi_R/2)]. \tag{2}$$

The fluctuation field $\boldsymbol{B}$ is analytically solvable:

$$B_\parallel(\theta) = -\int_0^\theta \frac{\sqrt{\pi}\, e^{\chi_R \sin^2 \kappa} \mathrm{Erf}(\sqrt{\chi_R} \sin \kappa)}{2\sqrt{\chi_R}} \mathrm{d}\kappa, \tag{3a}$$

$$B_\perp(\theta) = \int_0^\theta \frac{F_D(\sqrt{\chi_R} \cos \kappa)}{\sqrt{\chi_R}} \mathrm{d}\kappa, \tag{3b}$$

where $F_D(z)$ is the Dawson–F integral function: $F_D(z) = e^{-z^2}\int_0^z e^{y^2} \mathrm{d}y$.

The swim diffusivity is generated by the orientational fluctuation $\boldsymbol{B}$, propagated from the $\boldsymbol{q}$ space to the $\boldsymbol{x}$ space by the swim velocity $U_0 \boldsymbol{q}$:

$$\hat{\sigma}_\parallel^{swim} = \frac{D_\parallel^{swim}}{U_0^2/2D_R} = 2\int_{-\pi}^{\pi} B_\parallel(\theta) P_0^\infty(\theta) \cos\theta \mathrm{d}\theta, \tag{4}$$

$$\hat{\sigma}_\perp^{swim} = \frac{D_\perp^{swim}}{U_0^2/2D_R} = 2\int_{-\pi}^{\pi} B_\perp(\theta) P_0^\infty(\theta) \sin\theta \mathrm{d}\theta. \tag{5}$$

The detailed solution and asymptotics can be found in [12] and in the supplemental material (SM) available online at stacks.iop.org/NJP/20/053056/mmedia.

The double integrals are numerically integrated and shown in figure 2. Here $\hat{\sigma}_\parallel^{swim}$ and $\hat{\sigma}_\perp^{swim}$ are dimensionless functions representing the effects of χ_R:

$$\frac{\boldsymbol{\sigma}^{swim}}{-nk_s T_s'} = \hat{\sigma}_\parallel^{swim} \hat{\boldsymbol{H}}\hat{\boldsymbol{H}} + \hat{\sigma}_\perp^{swim} \hat{\boldsymbol{H}}_\perp \hat{\boldsymbol{H}}_\perp, \tag{6a}$$

where $\hat{\boldsymbol{H}}_\perp \hat{\boldsymbol{H}}_\perp = \boldsymbol{I} - \hat{\boldsymbol{H}}\hat{\boldsymbol{H}}$.

In the weak and strong field limits ($\chi_R \to 0, \infty$), the behaviors can be calculated with a regular expansion or Kramer's hopping theory [13], respectively. In the limit $\chi_R \to \infty$ the diffusivities and stresses are very anisotropic:

$$\hat{\sigma}_\parallel^{swim} \sim \frac{\pi}{2}\frac{e^{\chi_R}}{\chi_R}, \quad \hat{\sigma}_\perp^{swim} \sim \frac{1}{2\chi_R^2}; \tag{7}$$

the anisotropy, $\hat{\sigma}_\parallel^{swim}/\hat{\sigma}_\perp^{swim} \sim \pi\chi_R e^{\chi_R}$, grows exponentially with the field strength $\chi_R = \epsilon/k_B T$. The exponential growth reflects the Kramer's hopping process: at high χ_R a particle is trapped in either the $\pm\hat{\boldsymbol{H}}$

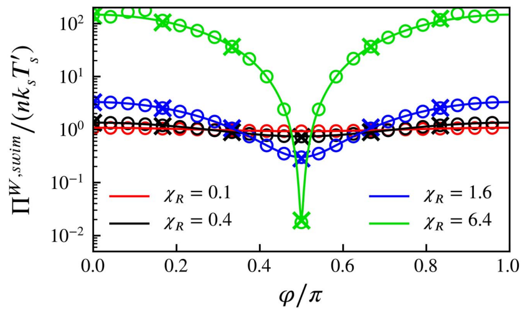

Figure 3. The comparison between the colloidal perspective, the continuum mechanics tensorial perspective, and Brownian dynamics simulations. The solid lines are calculated analytically from (8), the open symbols are calculated from (9) via a FEM solver with $(\delta/\ell)^2 = 0.2$ and $L = 20\ell$. The cross symbols are measured from particle-wall collisions in Brownian dynamics simulations with $\ell = 4a$ and $\delta = 0$ in a box with $L = 128a = 32\ell$ and periodic in the horizontal direction.

direction and requires a thermal fluctuation in orientation in order to overcome the barrier and flip to the other direction. The derivation of (7), utilizing Kramer's theory, is available in the supplementary material.

The 'divergence' of $\hat{\sigma}_{\|}^{\text{swim}}$ with χ_R does not imply that the force on the boundary is infinite. The continuum stress is $\boldsymbol{\sigma}^{\text{swim}} = -nk_s T_s' \hat{\boldsymbol{\sigma}}^{\text{swim}}$, where n is the bulk number density far from the boundaries. When $\chi_R \to \infty$, the ABPs will be trapped on the top or the bottom walls in figure 1 no matter how wide or narrow the domain, and the bulk number density n approaches zero, as the total number of particles in the domain is fixed and finite. The dimensionless stress $\hat{\sigma}_{\|}^{\text{swim}}$ 'diverges', but the net force on a wall is finite. This will become clear when the accumulation boundary layer structure is discussed in the next section.

From the tensorial continuum perspective, we can *analytically* calculate the pressure on the wall for any φ:

$$\frac{\Pi^{W,\text{swim}}}{nk_s T_s'} = \hat{\sigma}_{\|}^{\text{swim}}(\hat{\boldsymbol{H}} \cdot \boldsymbol{n})^2 + \hat{\sigma}_{\perp}^{\text{swim}}(\hat{\boldsymbol{H}}_{\perp} \cdot \boldsymbol{n})^2. \tag{8}$$

3. The colloidal (microscopic) perspective

Owing to symmetry, we only need to solve the Smoluchowski equation in the domain $z \in [0, L]$, $\alpha \in [-\pi, \pi]$, with the boundary conditions being non-penetrating at $z = 0, L$ and periodic in α. The angle φ is a parameter. All lengths are non-dimensionalized with $\ell = U_0 \tau_R$, and time is scaled with τ_R; thus,

$$\frac{\partial P}{\partial t} + \frac{\partial}{\partial z} j_T + \frac{\partial}{\partial \alpha} j_R = 0, \tag{9}$$

where $j_T = \cos\alpha P - (\delta/\ell)^2 \partial P/\partial z$ and $j_R = \chi_R \sin 2(\alpha - \varphi)P - \partial P/\partial \alpha$. These equations can be easily solved with a finite element PDE solver with non-penetrating boundary conditions on the top and bottom walls as illustrated in figure 1. We used the software package FreeFEM++ with automatic mesh refinement. After the steady state is reached, the swim pressure on the wall can be calculated as: $\Pi^{W,\text{swim}} = (n^W - n)\zeta D_T$, with $n^W = \int P(z = 0, \alpha)\mathrm{d}\alpha$.

In addition to the Smoluchowski colloidal perspective of the swim pressure, we also perform BD simulations to verify both the colloid and continuum tensorial perspectives. In the BD simulations, the pressure is determined directly as a summation of all the forces exerted by each particle-wall collision. In both cases we set n as the number density in the center of the channel; since the channel is wide enough to eliminate confinement effects n is the uniform *bulk* number density used in the continuum derivation of the swim diffusivity and pressure.

The comparison of the two different perspectives, together with results of BD simulations, is shown in figure 3. All three methods agree with each other.

The pressure calculated from (8) is analytic and is valid for arbitrary ratio of swimming to diffusion, $\ell/\delta \in (0, \infty)$, and is also independent of the channel width L as long as no confinement effects are important, i.e. $\ell/L \ll 1$. The pressure from the colloid perspective is calculated for $(\delta/\ell)^2 = 0.2$, and $L = 20\ell$ to guarantee that there are no confinement effects [5]. The BD simulations are conducted with $D_T = 0$, in contrast to the cases involving FEM solutions. The different settings are chosen to improve accuracy. In the FEM solutions, if $\delta = 0$ there will be a singular boundary layer which cannot be resolved by the FEM mesh. While in the BD simulations a non-zero D_T induces a non-zero passive osmotic Brownian pressure $nk_B T$ with significant Brownian noise when measuring the pressure on the wall. The different settings of D_T do not matter because in

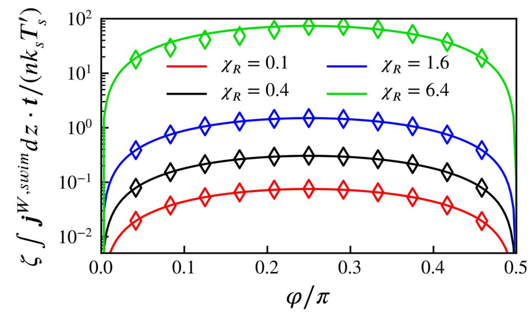

Figure 4. Comparison between the colloidal perspective and the continuum mechanics tensorial perspective for the shear component and the corresponding flow along the wall. The solid lines are calculated analytically from (10); the open symbols are data calculated with the colloidal perspective $U_0 \int \boldsymbol{m} \cdot \boldsymbol{t} \mathrm{d}z$ from the same FEM solution as in figure 3.

the ABP model D_T is not correlated with $\boldsymbol{D}^{\mathrm{swim}}$, and therefore does not affect $\boldsymbol{\sigma}^{\mathrm{swim}}$, nor our comparison between different approaches to predict the pressure on the wall.

The comparison clearly shows that the mechanical swim pressure on a wall satisfies the requirement of continuum mechanics, even when it is strongly anisotropic as shown for the case $\chi_R = 6.4$.

4. The tangential component

In continuum mechanics, $\boldsymbol{\sigma}^{\mathrm{swim}} \cdot \boldsymbol{n}$ is the traction on a plane with normal $\boldsymbol{n}$, and the tangential component $(\boldsymbol{\sigma}^{\mathrm{swim}} \cdot \boldsymbol{n}) \cdot \boldsymbol{t}$ in the tangential direction $\boldsymbol{t}$ is the shearing force applied on that plane, i.e., the friction between the two continuous media. For an anisotropic $\boldsymbol{\sigma}^{\mathrm{swim}}$, the tangential component is not necessarily zero.

However, there cannot be any shear force (friction) in the ABP model because the wall-swimmer interaction is excluded volume only; that is, a force is transmitted only in the normal direction to prevent the swimmer from crossing the wall. (In the ABP model hydrodynamics are neglected and thus there is no shear stress in the fluid.) When a swimmer swims towards a wall, it is trapped on the wall until the orientation $\boldsymbol{q}$ relaxes to a different direction so that it can leave the wall. In the absence of friction, the tangential component of ABP's motion, $U_0 \boldsymbol{q} \cdot \boldsymbol{t}$, is not transmitted to the wall; the swimmer 'slides' along the wall. Therefore, the tangential component of swim stress results in a net boundary *flow* of ABPs along the wall. The direction of the net flow is towards the left on the bottom wall and towards the right on the top wall for the $\hat{\boldsymbol{H}}$ shown in figure 1. The flow on the bottom and top walls are of the same magnitude but in opposite directions, and they cancel each other so there is no net overall motion in the domain and no net polar order.

For the 2D geometry shown in figure 1, the continuum tensorial stress perspective predicts the flow:

$$\frac{\zeta \int \boldsymbol{j}_T^{W,\mathrm{swim}} \mathrm{d}z \cdot \boldsymbol{t}}{n k_s T_s{}'} = (\hat{\sigma}_{\parallel}^{\mathrm{swim}} - \hat{\sigma}_{\perp}^{\mathrm{swim}}) \cos\varphi \sin\varphi. \tag{10}$$

It is clear that if $\chi_R = 0$, $\hat{\sigma}_{\perp}^{\mathrm{swim}} = \hat{\sigma}_{\parallel}^{\mathrm{swim}}$ and the flow varnishes; only 'normal stress differences' drive a flow. Here, $\int \boldsymbol{j}_T^{W,\mathrm{swim}} \mathrm{d}z$ has the dimension of the total flow rate along the boundary per unit boundary length (area if in the 3D case), while $\zeta \int \boldsymbol{j}_T^{W,\mathrm{swim}} \mathrm{d}z \cdot \boldsymbol{t}$ has the dimension of pressure.

Note that the stress difference driving the boundary flow is actually the total stress difference, $\sigma_{\parallel}^{\mathrm{tot}} - \sigma_{\perp}^{\mathrm{tot}}$, where $\boldsymbol{\sigma}^{\mathrm{tot}} = \boldsymbol{\sigma}^{\mathrm{swim}} + \boldsymbol{\sigma}^{\mathrm{osmo}}$, since the osmotic pressure is isotropic and cannot generate a normal stress difference.

From the microscopic colloid perspective, the swimmers form a kinetic boundary layer [5] on the wall. More specifically, there is net polar order $\boldsymbol{m} = \int P(\boldsymbol{x}, \boldsymbol{q}) \boldsymbol{q} \mathrm{d}\boldsymbol{q} \neq 0$ in the boundary layer close to the wall, even though the nematic orientation field generates no polar order in the bulk. By solving the Smoluchowski equation (9), the flow is obtainable by integrating m_t, the component of $\boldsymbol{m}$ parallel to the wall: $\int \boldsymbol{j}_T^{W,\mathrm{swim}} \mathrm{d}z \cdot \boldsymbol{t} = U_0 \int \boldsymbol{m} \cdot \boldsymbol{t} \mathrm{d}z$. More details about this boundary layer can be found in [12] and in the SM. The comparison between the colloidal perspective and the continuum mechanics tensorial perspective (10) for the tangential component, and the corresponding flow along the wall, is shown in figure 4; the agreement is excellent.

5. Conclusions and discussion

In this work we presented an example designed to extend the notion of the swim pressure to a true tensorial swim stress for the case of swimmers in a nematic orientation field. Swimmers under a nematic orientational potential show dramatically enhanced diffusion parallel to the field direction $\hat{\boldsymbol{H}}$, and significantly reduced diffusivity in the $\hat{\boldsymbol{H}}_{\perp}$ direction. This is in contrast to the polarization case [3, 6], where all swimmers are biased towards the same direction and the diffusivity in both the $\hat{\boldsymbol{H}}$ and $\hat{\boldsymbol{H}}_{\perp}$ directions decays algebraically with increasing χ_R.

The anisotropic swim diffusivity gives an anisotropic swim stress from the general relation between diffusion and stress: $\boldsymbol{\sigma}^{\text{swim}} = -n\zeta\boldsymbol{D}^{\text{swim}}$. Using a parallel-wall geometry, we showed that an anisotropic swim stress is a true stress in the continuum mechanical sense—the pressure on a boundary is $\Pi^{W,\text{swim}} = -(\boldsymbol{\sigma}^{\text{swim}} \cdot \boldsymbol{n}) \cdot \boldsymbol{n}$. This applies for anisotropic state, a state with polar order or one with nematic order.

In the absence of hydrodynamics, the tangential component of the anisotropic swim stress does not generate a shear stress (friction) but rather a net flow of ABPs along the wall. This is because the interaction between the ABP and the wall is assumed to be frictionless. From the continuum perspective the flow along the boundary is driven by normal stress differences. This is a generic feature of active matter systems. Due to confinement [5] or an orienting field, the stress in active matter is anisotropic. If the boundary orientation does not coincide with the principle axes of the swim stress tensor, net boundary flow will result. In the presence of hydrodynamics, this flow of swimmers along the wall would drag fluid with it and result in a shear stress. Recently, Burkholder and Brady [14] analyzed the effect of hydrodynamics on the pressure on the wall and found that hydrodynamic interactions may increase the swim pressure because the reduced mobility of the swimmers near solid boundaries results in an increased accumulation of particles over the no-HI case discussed in [5]. The quantitative effects of hydrodynamics on both the normal and tangential component of the stress in cases with orientational order requires further study. In particular, the vorticity generated by the fluid shear stress will affect the orientation distribution near the wall and thus the anisotropic swim stress.

It is not yet clear whether the swim stress can be treated generally as a true tensorial stress for arbitrary externally imposed orientational motion beyond the nematic ordering case discussed in this work. Rigorous mathematical proof requires solution of the kinetic boundary layer with arbitrary orientational order, which is difficult in general. The orientation moment expansion method [5, 10, 15] may be a possible route towards a general proof, but it is subject to proper orientation closure relations. We leave this for a future study.

The continuum tensorial perspective of swimmers has more profound use than simply to estimate the pressure on a flat wall for swimmers without net motion. Although there has been some debate as to whether the anisotropic swim stress can be an equation of state [9, 16–18], in this work we showed that from a purely mechanical perspective the anisotropic swim stress can be self-consistent and useful in predicting the surface forces. In a general mechanical transport problem such as sedimentation or active micro-rheology, the motion and deformation of swimmers on the length scale larger than $U_0\tau_R$ and timescale longer than τ_R can be simply solved with the continuum mechanics flux driven by the divergence of the tensorial total stress, the body force, and the swim force [3]. The boundary conditions for this large-scale transport equation must be properly constructed from the detailed near-wall dynamics on the small scale. This is similar to rarefied gas dynamics, where the non-continuum effects must be resolved on the scale of a few mean free paths at the boundary, and then a proper boundary condition for Navier–Stokes equation in the outer region can be constructed from the 'inner' solution. A similar outer-inner matching scheme also applies for ABPs, as discussed in our previous work on the curved kinetic boundary layer of active matter [10].

Acknowledgments

This work is supported by NSF CBET-1437570. We also thank the support from Simons Foundation, Flatiron Institute.

ORCID iDs

Wen Yan https://orcid.org/0000-0002-9189-0840

References

[1] Rusconi R, Guasto J S and Stocker R 2014 *Nat. Phys.* **10** 212–7
[2] Kaya T and Koser H 2012 *Biophys. J.* **102** 1514–23
[3] Yan W and Brady J F 2015 *Soft Matter* **11** 6235–44
[4] Takatori S C, Yan W and Brady J F 2014 *Phys. Rev. Lett.* **113** 028103
[5] Yan W and Brady J F 2015 *J. Fluid Mech.* **785** R1
[6] Takatori S C and Brady J F 2014 *Soft Matter* **2014** 9433–45
[7] Coffey W T and Kalmykov Y P 2012 *J. Appl. Phys.* **112** 121301
[8] Ezhilan B, Alonso-Matilla R and Saintillan D 2015 *J. Fluid Mech.* **781** R4

[9] Solon A P, Fily Y, Baskaran A, Cates M E, Kafri Y, Kardar M and Tailleur J 2015 *Nat. Phys.* **11** 673–8
[10] Yan W and Brady J F 2018 *Soft Matter* **14** 279–90
[11] Frankel I and Brenner H 1989 *J. Fluid Mech.* **204** 97–119
[12] Yan W 2016 Dynamics of chemically active suspensions *PhD Thesis* California Institute of Technology https://doi.org/10.7907/Z9Z60M1V
[13] Kramers H A 1940 *Physica* **7** 284–304
[14] Burkholder E W and Brady J F 2018 *Soft Matter* **2018** 3581–9
[15] Saintillan D and Shelley M J 2015 Theory of active suspensions *Complex Fluids in Biological Systems* ed S E Spagnolie (Berlin: Springer) ch 9 pp 319–55
[16] Hagen B, Wittkowski R, Takagi D, Kümmel F, Bechinger C and Löwen H 2015 *J. Phys.: Condens. Matter* **27** 194110
[17] Ginot F, Theurkauff I, Levis D, Ybert C, Bocquet L, Berthier L and Cottin-Bizonne C 2015 *Phys. Rev.* X **5** 011004
[18] Junot G, Briand G, Ledesma-Alonso R and Dauchot O 2017 *Phys. Rev. Lett.* **119** 028002